MODELING OF BRAGG REFLECTORS TO INCREASE PERFORMANCE OF HIGH EFFICIENCY III-V MULTIJUNCTION SOLAR CELLS

by

Mikayla Allyson Bradsby

A thesis submitted to the Faculty and the Board of Trustees of the Colorado School of Mines in partial fulfillment of the requirements for the degree of Master of Science (Applied Physics).

Golden, Colorado

Date _____

Signed: _____

Mikayla Allyson Bradsby

Signed: _____

Dr. Eric Toberer
Thesis Advisor

Golden, Colorado

Date _____

Signed: _____

Dr. Fredric Sarazin
Department Head Title
Department of Physics

ABSTRACT

High efficiency III-V solar cells are important for solar concentrator systems and space applications. To increase the efficiency of these cells, creative methods have been employed such as adding quantum wells in stress-balanced superlatticies to get closer to the ideal bandgaps for three junction cells. However, due to the strain of the quantum wells leading to limited possible growth thickness this addition of quantum wells is insufficient to completely absorb light in the regime they are designed to absorb. This work details modeling work done on Bragg reflectors in between the second and third subcells of a three junction device, behind the quantum wells in an attempt to increase efficiency in the range of the quantum wells. Modeling to increase the power to the second and third subcells using genetic algorithms was found to increase the overall power of these two subcells. This entails increasing the absorbance and therefore power of the second cell while keeping transmission high in the range of the final subcell. This is a challenge because in traditional Bragg reflectors the peak reflectance is proportional to the sidelobe reflectance that decreases power to the final subcell. Other optimization techniques such as optimizing for reflection profiles and current were also attempted but were found to be less useful due to imprecise or lesser abilities to account for the impact on the bottom subcell which turned out to be very significant. As such, it was found that the Bragg reflectors designed were only helpful when the open circuit voltage (Vop) of the final subcell was low or the absorbance of the quantum wells was high, when loss to the bottom subcell was either less significant.

TABLE OF CONTENTS

LIST OF FIGURES

LIST OF TABLES

LIST OF ABBREVIATIONS

Anti-Reflection Coating	ARC
Closed Circuit Current	Jsc
External Quantum Efficiency	EQE
Multiple Quantum Wells	MQW
Open Circuit Voltage	Vop
Photovoltaics	PV
Quantum Efficiency	QE
Quantum Wells	QW

ACKNOWLEDGMENTS

I would like to thank and acknowledge Jeronimo Buencuerpo, Ryan France and Myles Steiner for being excellent mentors to me and helping me enter the world of research. Their time and support have been invaluable to me. Additionally Eric Toberer's advice and willingness to help me find creative solutions has been extremely helpful. I would also like to think my family for their constant support, encouragement and patience. And finally I would like to acknowledge my friends, especially Forrest, Jewel, Grant and Maddie for having my back and bringing me the joy I needed to get through the writing of this thesis.

CHAPTER 1
INTRODUCTION

High efficiency solar cells are important for applications in space and terrestrial solar concentrator systems. Commercial cells are typically silicon based as silicon is a cheap and abundant semiconductor. However, semiconductors formed from elements in the third and fifth period of the periodic table (III-V materials) are more expensive but tend to be more efficient materials for solar cells.[1] In space applications minimizing the weight of solar cells is crucial for energy conservation and cost efficacy. Improving efficiency allows more energy to be produced for a constant amount of material.[2] For concentrator system applications the overall cost is dominated by factors outside the cell itself such as the mirrors and mechanical structures to support them. Since the cost of the cell is a smaller factor it is beneficial to improve the efficiency since the gain in power produced is more significant than the increase in cost.[1] While there are cost factors that make high efficency cells more viable in these sectors,it is possible that in the future these will not be the only sectors that III-V based solar cells dominate in. Further cost saving innovations could allow them to compete with Si cells for widespread commercial and residential operation.[3]

The fundamental structure that has been used to achieve non-concentrator multijunction high efficiency cells is a three junction cell with a Gallium Indium Phosphide (GaInP) top subcell, a Gallium Arsenide (GaAs) middle subcell, and a Gallium Indium Arsenide (GaInAs) bottom subcell.[4] The purpose of layering these cells is that each one has a different bandgap. These materials cannot absorb light below the bandgap but energy absorbed above the bandgap is lost as heat(thermalization). Having the solar spectrum absorbed in three different regions allows for an increased efficiency and lessens thermalization loss, while still capturing most of the solar spectrum.[5] A 37.9% efficiency has been previously obtained using a 3 junction cell measured under the 1-sun global

spectrum. [6] This dissertation describes a novel approach to increase the absorption of the middle junction as a part of a project to develop a cell with a record efficiency of 40%.

An approach that has been established to increase efficiency was to use quantum wells to decrease the bandgap of the middle subcell(primarily composed of GaAs) to be more similar to the theoretic ideal described by Olson and Friedman.[5] It is possible to mathematically calculate the ideal bandgap for each cell but there is no guarantee that a material with that bandgap and all other material properties desired will be available. Creative solutions like adding quantum wells have been used to get closer to this mathematically ideal bandgap. This decrease in bandgap was accomplished by growing alternating layers of GaInAs and GaAsP on the middle subcell. GaInAs has a lower bandgap and so was the primarily desired material, while GaAsP is used to minimize the difference in lattice between the GaAs and GaInAs.[7] The 10.33 nm GaInAs region was sandwiched between two 11.07 nm barriers of GaAsP. Initially there were 50 of these quantum wells modeled, leading to a total thickness of 1.62 microns, corresponding to a quantum efficiency around 0.4. However, the extended bandgap created by GaInAs and GaAsP does not have as high of a quantum efficiency as the rest of the cell. Since each layer has a different lattice constant, this combination of layers cannot be grown thick enough to absorb most of the light without the strain from the interfaces being significant enough that defects are introduced. Additionally because these alternating layers create quantum wells the electrons will not diffuse out of the quantum well region they must be grown in the depletion region where there will be an electric field to move the excited electrons. This also creates limits on the total thickness that leads to lower overall absorbance. In order to address this lower absorbance, these layers were kept at a thickness that could tolerate the strain and a reflector structure was added in an attempt to increase the lower absorbance in this region. [8]

Increasing the thickness is not the only way to increase the amount of time light spends in a material (and therefore the chance it has to excite an electron). Adding a perfect

reflector, and therefore allowing photons another "lap" across the material, can in ideal cases double the optical path length. One solution could then be adding a reflector after the quantum wells to increase absorbtion.

A reflector to target the region of the quantum well would be more effective if it were grown immediately after second subcell but was still transmissive for the photon energies that the third subcell was most efficient in absorbing. Distributed Bragg Reflectors(DBRs) are used in this work to accomplish this.

DBRs are dielectric and semiconductor reflectors that use Snell's law and constructive and destructive interference to reflect light at a given wavelength.[9] This makes them promising for use in increasing the quantum efficiency in the wavelength range of the quantum wells, as they can be targeted to have a high reflectivity only in the range where the most significant improvement is needed. If the cells were all optically thick then light from the sun would pass through the cell, the highest enegry photons would be absorbed in the high bandgap top subcell, then all photons with insufficient energy to excite electrons in that cell would pass onto the middle bangap middle subcell, and all photons with insufficient energy to excite electrons in that subcell would pass onto the low bandgap bottom subcell. However, since the quantum wells are not optically thick, some light with sufficient energy to generate electricity in the middle subcell will pass though to the bottom subcell, and the excess energy will result in thermalization loss. [5] As a result the Bragg reflector was grown after the quantum wells but before the final subcell.

Bragg reflectors are effective here as they are able to be grown so that the main peak is only in the range of the quantum wells, allowing for the reflected light to be absorbed by the quantum wells without undue disruption to the light absorbed in the third subcell.

In general distributed Bragg reflectors work by reflecting light at 1/4 wavelength intervals to create constructive interference.[8] Since this is dependent on one wavelength, this leads to one strong peak at the target wavelength and then due to higher order interference there are smaller peaks called sidelobe reflection. As shown in figure Figure 1.1

This sidelobe reflection reflects light with longer wavelengths that could otherwise be absorbed in the third subcell.

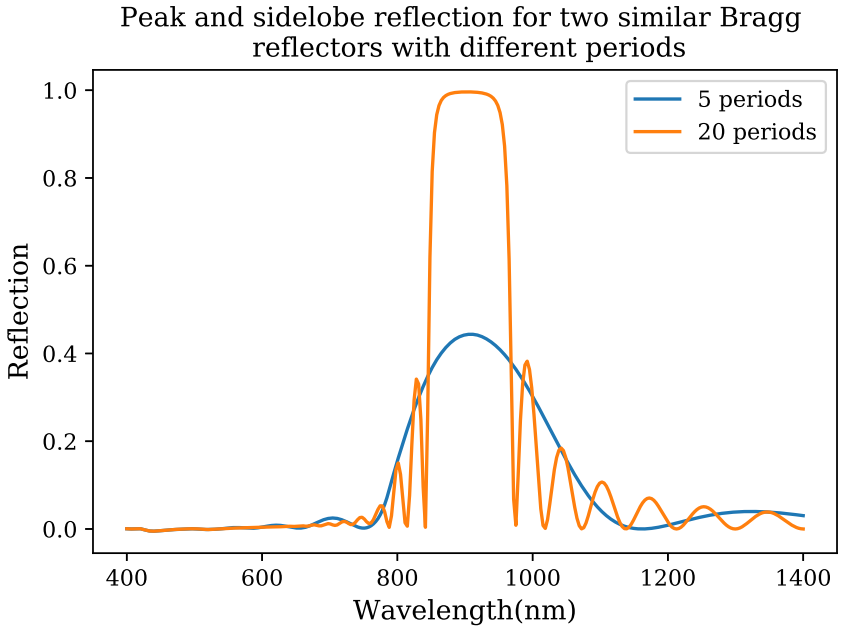

Figure 1.1 Peak and sidelobe reflection in sample distributed Bragg reflector

Since the DBR is between the second and third subcells, it is important that the transmission is maximized in the range of the third subcell, in addition to reflecting light into the quantum wells. Therefore, the ideal design is one that has high reflection in the range of the quantum well and no reflection at longer wavelengths. However, in standard DBR designs, generally the higher the peak reflection, the higher the reflection off the central peak(the sidelobe reflection). Therefore, the challenge presented in this work is to create a DBR that is able to increase the reflection and power in the central subcell without decreasing the overall benefit by reflecting light away from the final subcell. Since in the standard formulation of the Bragg reflector these two things go hand in hand, the difficulty is finding ways to preserve the Bragg reflector structure enough that it functions as a Bragg reflector but is different enough that we are able to work around this correlation. In order to achieve this goal, genetic algorithms are used on structures similar to basic Bragg reflectors to try to find Bragg reflectors that enhance the power of these

cells and models were developed and tested to better understand the impact of changing the Bragg reflector and specific cell design parameters.

CHAPTER 2

BACKGROUND

High efficiency solar cells are important both in concentrated solar systems and for powering satellites, probes and other spacecraft.[10] Silicon based solar cells are currently more pervasive for commercial applications due to their lower cost but are limited in terms of efficiency. III-V materials are a higher efficiency alternative. III-V materials are semiconductors composed of elements in the group III (like Aluminum, Gallium, Indium) and group V(like Phosphorus and Arsenic) of the periodic table. While Si is in general cheaper than higher efficiency III-V materials by volume, the higher efficiency of III-V materials makes them more cost effective in terms of cost per power in concentrator systems. [1] Their higher efficiency makes them favorable in space where launch costs mean that weight is paramount. [4]

In this chapter I present a summary of topics related to the experiments and modeling work done in chapter 4 and their importance to that work. In particular I discuss the cell structure, how quantum wells work for multijunction solar cells, what Bragg reflectors are and how they work, and what models were used and the theory behind them. Since the modeling required a few different types of models and processes, the discussion of the models are broken down into the materials, the structure, and the optimization of the Bragg reflector on the cell structure. The calculations used to extract information from these models are also explained.

2.1 Cell Structure

Since III-V materials are currently used in applications where efficiency is prized, a number of structures have been grown with these materials to optimize the overall cell efficiency. Multijunction cells have been conceptualized to be a more efficient structure for making III-V solar cells than the standard single junction cells for over 50 years.[11] These

multijucntion cells are made up of multiple junctions, also called subcells, each made of distinct materials. These materials are stacked on top of each other in order of decreasing bandgap with window and tunnel junctions between for an overall more efficient cell.

Multijunction cells are more efficient as they take advantage of different materials having different bandgaps. Energy less than the bandgap is not absorbed and excess energy above the bandgap is dissipated as heat. It is possible to capture some of the benefits of multiple bandgaps by creating solar cells with multiple materials at varying bandgaps. [5] In fact,Henry's work shows that by adding only a few new subcells much of the multi-bandgap advantage can be achieved, as with each additional bandgap added, the rise in efficiency declined. [12]

Each of the junctions in the multijunction cell are stacked from highest to lowest bandgap. Since light cannot be absorbed beneath the bandgap, this means that if all cells absorbed 100% of the light, light would pass through the stack and be absorbed by the junction where it would be most efficiently converted into electricity. It is possible to model the efficiency based off of the bandgaps and find the maximum efficiency of the combined cell based on the band gap of each. Not all light will be absorbed in the cell where it will have maximum efficiency because absorbance is ultimately a function of the optical thickness of the cell. The optimal wavelengths for each cell are dependent on the solar spectrum used and the material properties of each of the cells components.[5] The absorbent subcells are only one of many critical components in the overall multijunction stack. Another of these components are window layers, which are layers above the absorber layers that minimize interference to cell function from phenomenon on the surface of the subcells. In the words of Olson, Friedman and Kurtz they exist to "passivate the surface states associated with the emitter surface."[5] In order to be an effective window layer the material needs to be high quality, have a lattice constant close to its nearest material, have a much higher bandgap, a large valence-band offset and high electron concentration An additional component that was modeled was the tunnel junction. Tunnel junction are used

to provide "low-resistance connection" between the subcells. These are optically transparent as to not interfere with the subcells but still provide electrical conductivity. [5] There are also anti-reflection coatings on the surface of the overall cell. These anti-reflection coatings help to minimize the reflective losses from the light hitting the cell.

2.2 Quantum Well

An individual quantum well is essentially the physical version of the finite potential well commonly found in Quantum Mechanics classes. In creating a small region with a lower potential than the regions on either sides, the electrons in the conduction band are confined to a series of discrete energy states. However, as the quantum well has finite potential it is possible for the electrons to leave the quantum well. They do this in two main ways, thermonic emission or tunneling. Thermonic emission is when thermal energy allows excited electrons to escape the wells and swept into the electric field of the cell. Tunneling is when the thin barriers allows for the carriers to tunnel through the cell. [13] In a solar cell the quantum well structures commonly used to improve performance are stress balanced superlattices.

An individual quantum well can only have electrons at a few discrete energy levels. However, since electrons can tunnel between quantum wells within the superlattice these discrete energy levels combine to form bands of allowed electron energy.[13] These energy bands multiply and converge to bulk behavior the thicker they are. These stress balanced superlattices are useful in solar cells because while multijunction cells are most efficient when the component materials lie at specific bandgaps and there is no strain, there are no available single material semiconductors that fit these requirements and have an appropriate lattice constant. However, InGaAs does have a lower bandgap but does not have a lattice constant compatible with the rest of the GaAs cell. While the materials that make up the quantum wells have strain since it is a series of relatively thin layers and in a quantum well structure with GaAsP(P=0.098) and InGaAs(In=0.106), the compressive strain of this compound of InGaAs balances with the tensile strain of this compound

GaAsP leading to minimal enough average strain to not introduce dislocations for thin layers, and enough strain that the InGaAs bandgap changes to be closer to the ideal bandgap.[8] These materials are chosen because these specific ratios of the III-V materials have a lattice constant that when strained is close to the lattice constant of AlAs while keeping the InGaAs bandgap as close as possible to the ideal badgap. These quantum wells cannot be grown arbitrarily thick as the presence of strain creates morphology problems which will eventually lead to composition variation and dislocation formulation.

2.3 Bragg Reflectors

Reflectors are incredibly useful components in a solar cell as a perfect reflector of an optically thin cell could theoretically nearly double the absorption by giving photons that passed through a cell without being absorbed a second chance to do so after reflection. It is therefore an effective pathway to boost absorbance in a region that is lacking it, such as quantum wells. A Bragg reflector in particular is a "A periodic structure formed from multiple alternating layers of materials with different refractive index."[14] These Bragg reflectors are highly reflective at a specific wavelength. In their most standard form they do this by having each of the alternating material layers follow the equation n*d=i*lamda/4 where n is the index of refraction, d is the thickness and lambda is the target wavelength and i is any odd integer. [15] The reason this is an effective Bragg reflector is that when light enters the structure the light at the target wavelength will partially reflect and partially transmit, at the next layer it will also partially reflect and partially transmit. Because it reflects at a $\frac{1}{4}$ wavelength the light transmitted back constructively interferes, as this is repeated for many layers (the more layers the more effective the reflector) creating a very effective reflector at that wavelength.[14] However, as this is wavelength specific the reflection is only high for a limited range. There are also other, much smaller peaks on the side of the main peak, called sidelobes, where constructive interference occurs to a limited extent. Typically, a high index contrast is helpful in these sort of structures to promote a high ratio of reflection to transmittance.

2.4 Modeling Materials

The primary steps used in creating the models that were used in the rest of the process were, modeling the materials, creating a usable model of the cell, genetic optimization and modeling the current, voltage and power. In order to make usable materials we needed materials that we had a high degree of confidence in their optical properties. Materials that are commonly used for these sorts of applications have been measured and are accessible for these models. However with materials like $Al_xGa_{1-x}As$ where there are theoretically infinite variations depending on the relative composition of Al to Ga it is impractical to grow and measure enough of these variants to be useful to the modeling process. Vurgaftman, Meyer and Ram-Mohan describe a method for using the band parameters of zinc blende crystals (of which AlGaAs is) to find properties of the materials (such and energy bands and effective mass) as a function of a few parameters that can be measured and modeled. Specific permutations of $Al_xGa_{(1-x)}As$ are modeled allowing for the calculation of material properties for any given x in $Al_xGa_{(1-x)}As$. [16]

Once a solid material model has been established, the next step is to use these materials to create a usable model of the cell. Pyphotonics,is a python library created by Jeronimo Buencurepo that was used to model the reflection,transmission and absorption. [17] This library used rigorous coupled wave analysis (RCWA) to find these elements. RCWA is a numerical approach to solving Maxwell's equations for a layered stack of materials. Vertically these materials can have a given thickness but are assumed to be infinite in the direction perpendicular to the light. Since this does not change the ratios of reflectance to absorbance to transmission this was a reasonable assumption. [17] To create a model that could be used, an actual cell (MQ689) was simplified to the most relevant components and replicated. MQ689 is a three-junction cell with quantum wells, and so the model is too. The model has a 2-layer Anti-Reflection Coating (ARC) of MgF_2 and ZnS, a window layer of 20 nm of AlInP, the top subcell is represented by a 2 micron thick slice of GaInP, then there are 200 nm of the AlGaInP and 20 nm of GaAs tunnel junction and 20

nm of GaInP that serve as the window layers before the middle subcell modeled as 2 microns of GaAs and then the quantum wells. Initially the quantum wells were modeled as a 1 micron thick slice of InP, as that has a similar absorption profile and so seemed like it would be similar enough to be functional. However this was proved to be untrue and so a more accurate model was implemented that has a well thickness of 10.3 nm of InGaAs with an Indium content of 0.106 and 22.14 nm barriers of GaAsP with a phosphorus content of 0.098.[18] While this dramatically slowed down the run time of the model with a visually similar EQE prior to the addition of the Bragg reflector, the change upon adding Bragg reflectors was much more intuitive and reasonable. The Bragg reflector is modeled after the quantum wells and the bottom cell is represented by a 20 nm layer of GaInP and a 2 micron layer of GaInAs. A bit of work with understanding the effect of the back reflector was done leading to multiple types back layers being used but unless stated otherwise there was a semi-infinite sheet of gold functioning as the back reflector. This overall structure is summarized in table Table 2.1.

Table 2.1 Structure of modeled Bragg reflector

Material	**Thickness (nm)**		**Purpose**
Air	Semi-infinite		Simulating the actual interface between cell and environment
MgF2	98		Anti-Reflection Coating
ZnS	48		Anti-Reflection Coating
AlInP	20		Window Layer
GaInP	2000		Top Cell Absorber
AlGaInP	200		Tunnel Junction
GaAs	20		Tunnel Junction
GaInP	20		Window Layer
GaAs	2000		Middle Cell
GaAsP	11.07	x#QW	Alter Bandgap of middle cell to be more favorable
GaInAs	10.33		
GaAsP	11.07		
Bragg Reflector	Depends		Increase the reflection into the QW regime to increase absorption
GaInP	20		Window Layer
GaInAs	2000		Back Subcell
Au	Semi-Infinite		Back Reflector

While this structure remained mostly the same throughout the experiments, the Bragg reflector was changed and optimized. This was mostly done through either varying the reflectors off of a known design or through genetic optimization. The library NLOPT was used to do this genetic optimization. NLOPT is "a free/open-source library for nonlinear optimization." This software has a wide variety of optimization routines that are callable.[19] The primary method that I used was controlled random search(CRS) with local mutation. NLOPTS implementation is based off of P. Kaelo and M.M. Ali's paper "Some Variants of the Controlled Random Search Algorithm for Global Optimization." This paper describes a method where properties of the function are unnecessary, rather the only requirement is that the function can be computed for all values in the sample space. This system works by forming a set of points distributed throughout the sample space. New points are tried using the Nedler and Mead algorithm and if its better as defined by the input parameters the new point is added to the set of points and the worst point is removed. This occurs until a stopping condition is reached. [20] (In our case this was a number of iterations after which the new points were consistently within a small margin of error to each other) Kaelo and Ali propose a few different additions to increase the convergence, the one implement in NLOPT is one in which if a trial point is worse than the existing points, other "local mutations" of this trial point are also attempted to explore the local space and then the simulation moves forward. This minimizes the problem that this sort of optimization tends to have of potentially missing solutions as there is no guarantee that any of the solutions tried will be the optimum.[19] The other optimization used with NLOPT was the ESCH which is an evolutionary algorithm. The evolutionary algorithm works by mimicking evolutionary strategies in creating an initial set of potential values in the space, taking the values closest to the figure of merit and combining them and adding "mutations" and replacing the worst elements of the previous population with the best elements of the recombination result. Figure 2.1 illustrates this process.[21]

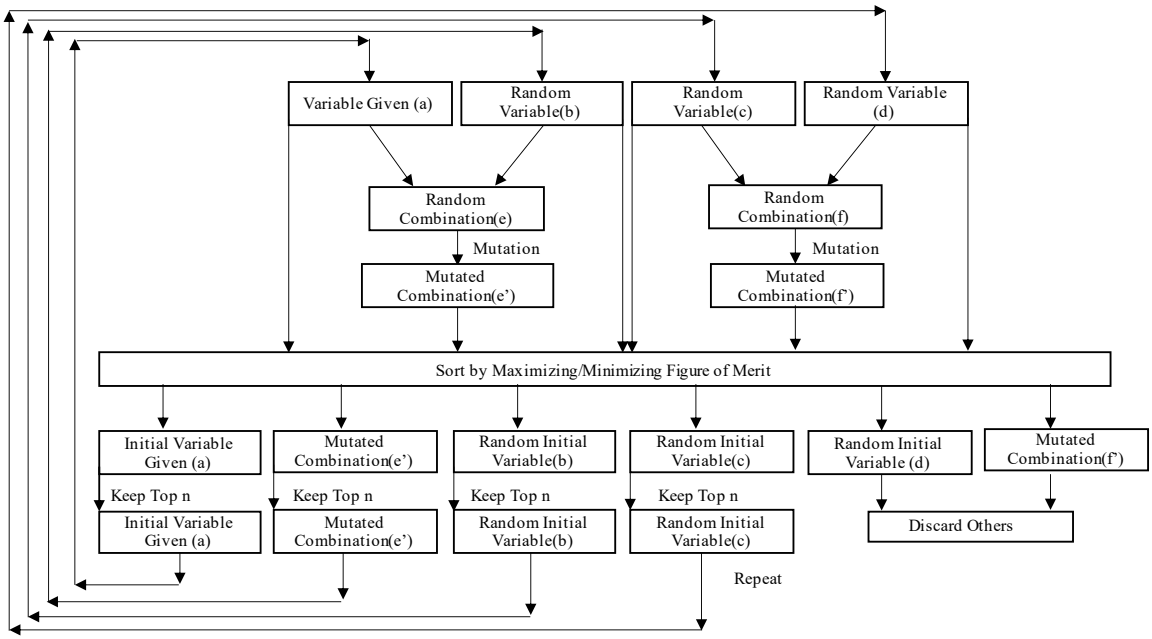

Figure 2.1 Evolutionary algorithim process of optimization

2.5 Understanding Results Of Models

The end result of these models are a series of input parameters and the calculation of the figure of merit. In order to gain physical meaning of these more advanced than reflection profiles there was some amount of math that had to be done. The easiest of these is the quantum efficiency. Pyphotonics is able to produce the overall reflectance, transmittance and absorbance as well as the absorbance for any set of layers. Quantum efficiency is the ratio of carriers collected to the number of photons incident on the cell, and absorption describes what percentage of incident light is converted into other forms of energy inside the material (such as phonons ore exiting electrons). Absorption provides a good model for this quantum efficiency under the assumption that all light absorbed perfectly converts to carriers collected. In practice this is not true but since we are interested in the optical rather than the electronic properties primarily and are only comparing against other models with the same assumption it is an effective model for those purposes. The current is then able to be calculated because it is the integral of the

quantum efficiency times the solar spectrum. Given the current it is then possible to find the power using P=I*V*FF where P is the power, I is the current, V is the voltage and FF is the fill factor that relates how much power there is ideally to how much power there actually is for a system. The current is able to be found from the absorbance and the voltage is a known quantity based on the band gap.The reflectance and absorbance from pyphotonics and the quantum efficency, current and power can then be used to analyze the effacy of the Bragg reflectors produced.

CHAPTER 3

METHODS

A primary goal of project was to understand how various parameters impacted the Bragg reflector and then use different optimization structures and regimes to attempt to learn more about how these structures interact and to increase the performance of the cell.

3.1 Understanding Basic Parameters That Impact Bragg and Cell Design

In order to gain a better intuition and understanding of the "dials" that impact Bragg and cell design and to validate the models consistency with theory, a series of models were run slightly varying the most important parameters to vary. A given model was input into the function and then a single aspect of it was varied a number of times, the reflection profile was then calculated using RWCA via pyphotonics and these reflection profiles were compared. This single model was a 60 layer Bragg reflector with 30 repetitions of alternating 63.0 nm of $Al_{0.1}Ga_{0.9}As$ and 75.5 nm AlAs. To test the impact of the change of the thickness of each layer, the width of each was increased and decreased in ten nm increments until this thickness either stopped being physically meaningful or the total variation reached 30 nm from the original value. Theoretically, as the number of layers of a Bragg reflector increases, each additional layer will have a less significant impact on the overall structure as fewer and fewer photons reach the final layer. To quantify how this change occurred in a Bragg reflector with two repeating layers, the total number of repetitions was increased one at time. In another series of models the composition was changed by up to thirty percent by plus or minus five percent, plus or minus ten percent and plus or minus twenty percent. To understand the impact of the thickness of the QW layers, the number of QW layers was modeled at 10,50,100,150,200 and 300 layers with both gold and nickel back reflectors.

3.2 Understanding Impact of Voltage and Number of Quantum Wells on Cell Power

As genetic optimization was used, it was found that solutions generally did not converge in the quantum well region. Rather, the peak reflection was closer to 825 nm(where the properties of GaAs dictate the absorbance), meaning that the Bragg reflectance was improving the absorbance in the GaAs subcell rather than in the quantum wells. The optimization converged around 825 nm because using the calculated open circuit voltage(Vop) of 0.75 V(which told us the maximum voltage) with 50 quantum wells a Bragg in the quantum well region did not increase the power in the GaAs+QW subcell enough to sufficiently offset the loss of power from GaInAs in that same region. In order to investigate the parameters that would lead to this behavior, the current and power for the GaAs+QW and GaInAs subcells were calculated as a function of the Vop of the GaInAs and as a function of the number of quantum wells. Increasing the Vop changes the weighting of the GaInAs subcell which gives the power of the GaAs+QW more comparative importance. Increasing the number of quantum wells has a similar effect but for a different reason because doing so heightens the comparative importance of the GaAs+QW, not by changing the weighting factor directly but by changing where the absorbance of the 830-930 nm photons is the strongest.

3.3 Use of Different Figures Of Merit In the Genetic Algorithm

The figure of merit(FOM) is the most critical element in ensuring that the genetic algorithm converges to a useful result. In its most basic form, it was thought that finding the optimal Bragg reflector is a matter of finding a way to increase the reflection of the Bragg reflectors at bandgaps below the QW bandgap (1.35 eV) and maximizing it above.In order to start exploring the phase space which the Bragg reflectors could be optimized in, the first figure of merit optimized for Bragg reflectors that most resembled a step function with a maximum reflection above 1.3 eV therefore increasing the power of the GaInP and GaAs+QW subcells, and no reflection below 1.3 eV as to not impact the

performance of the GaInAs subcell. To do so the figure of merit minimized the difference between the Bragg reflector found by the optimization and a step function that was set at one between 350 and 850 nm(3.5-1.5 eV) and zero between 850 nm and 950 nm (1.5 and 1.3 eV). While this was theoretically the goal, standard Bragg reflectors work by maximizing reflection of a single central wavelength that drops off on either side. Trying to get that general form to fit a step function leads to some unexpected and impractical results. These results included high sidelobe reflection because everything was weighted equally and so, as far as the optimization was concerned, having high reflection was more beneficial overall, though this is not true in actuality. Additionally as far as this optimization was concerned a peak in reflection at 400 nm was equally helpful as a peak at 800 nm which does not acurately represent the desired outcome. The optimizations using this figure of merit also produced structures that did not resemble anything like the Bragg reflectors we expected.

In order to remedy this to an extent, the idea of increasing the reflection in the GaInP and GaAs+QW subcells and minimizing it in the GaInAs region was preserved but a weighting factor was added. This was accomplished by creating a figure of merit and integrating over the transmission in the range in the quantum well, and integrating for reflection in the range of the bottom subcell. This was then minimized such that there would be the greatest reflectance in the quantum well range and a minimized reflection in the GaInAs subcell. Weighting factors were added to each aspect of this for greater of control. This made the figure of merit Equation 3.1.

$$w_1 \int_{870}^{930} T + w_2 \int_{930}^{1400} R \tag{3.1}$$

This optimization serves the same end goal except that it was less computationally intensive and allowed for more control over what was deemed important. A few different weightings were tried (1:1, 50:1,100:1). This worked a bit better(partly because the conversion error was found and corrected for), but determining which would improve the cell performance was difficult because the relative importance of increasing the reflection

and minimizing the sidelobe reflection was not well understood. The plan was for the ratio of the weighting factors to be dialed in as an understanding of how it impacted the cell. Understanding how these parameters impacted the cell was done by optimizing on the current and power. Since these optimizations were independently useful there was no reason to revisit this original figure of merit.

The next figure of merit that was used was the current of the middle, GaAs+QW cell. In order to do so a model of the actual 3-junction cell had to be created, I used MQ689 as a reference. Figure 3.1 visually illustrates the modeled layers based on this cell.

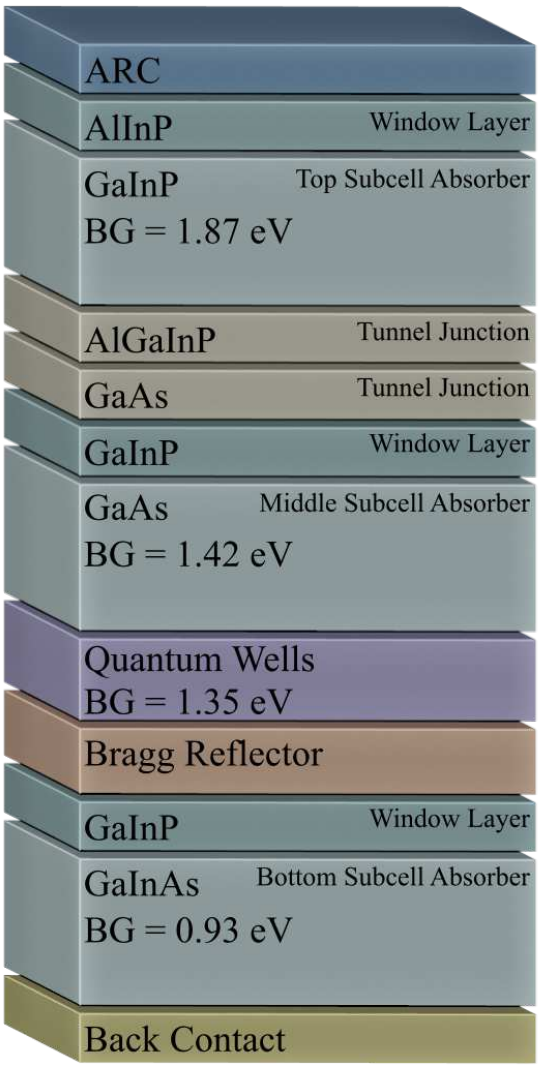

Figure 3.1 Visual structure of modeled cell based off of MQ689

Initially InP was used instead of a detailed quantum well model because it was significantly less computationally intensive but had a similar absorbance profile to the quantum well cells. It was hypothesized that increasing the absorption in the region of the InP should have the same impact on the current and power as a full quantum well model. Current increase was used as the main goal of this project was to increase the performance of the cell by increasing the absorbance and therefore current of the middle cell. Model optimization done with the goal of increasing current did produce an increase in current but a much smaller increase than we would have hoped for (a difference of $0.2\ \mathrm{mA/cm^2}$ instead of $2\ \mathrm{mA/cm^2}$) but overall had reasonable results.

This did not account for the loss to the back cell and so the next figure of merit used the maximum power of the middle subcell plus the maximum power of the bottom subcell as a figure of merit. This was an effective figure of merit since a bragg reflector essentially moves current from the lower subcell to the middle subcell where it will produce more power because of the larger bandgap and therefore higher voltage. Therefore power is an effective way to capture the benefit of the Bragg reflector.

As optimizing on power was somewhat successful so the next step was to refine the cell model to add in a more complete quantum well model, as our assumptions about the fidelity of the InP models seemed to be faulty, given the nearly insignificant response to back reflectors and Bragg reflectors. While the exact reasons were not examined it could be due to the fact that the method used to calculate the absorption and reflection relied on the index of refraction and the interfaces between layers. While InP has a similar overall bandgap and therefore some important similar material properties it lacks the same subtlety in the number of layers and has nonidentical complex indices of refraction. This new model was used with an algorithm that maximized the power of the bottom two subcells (the only two that were impacted by the addition of the Bragg reflector).

3.4 Using Different Structures For Bragg Reflectors

While it is theoretically possible to model a Bragg reflector by creating a set number of layers and letting the thickness and composition of each layer vary arbitrarily, and in fact this was attempted, it is impractical for quick convergence. By default the Bragg modeled was 60 layers thick and so if each layer had an individual thickness and composition there are 120 variables. The material for the Bragg was chosen to be $Al_xGa_{1-x}As$ and the model we used for this material allowed x to vary between zero and one in increments of 0.01. This means that there are 100 meaningful distinct options for each of these variables. While the range of thicknesses allowed was varied, the final range reached was between 40 and 100 nm and so if we assume that any difference less than one nanometer is not distinct enough to warrant being counted as its own solution that's still 60 possible options. With these estimates that's 6000 options per layer and at 60 layers is 10^{226} options. While genetic algorithms are effective at dramatically parsing down the number of solutions attempted that still takes an intense amount of computational time to go through. This is especially true if you consider that the algorithm has no way of knowing that a thickness of 70.000001 nm is no different for our purposes than 70 nm so while there may be around 10^{266} functionally different solutions, the algorithm has many more options to try. These large number of variables pose two problems, the first of which is with such a large number of variables and an algorithm that iteratively improves and so cannot be run in parallel the computational time is immense. The other problem is that such a small fraction of the options are anything like a Bragg reflector so the number of useful iterations is extremely small and finding them becomes an even more daunting task. Fortunately, that second issue gives rise to a solution to the first. If some amount of Bragg-like structure is enforced on the model the number of iterations is greatly reduced and the speed to find a reasonable reflector is greatly increased. The simplest technique to do so is to constrain the Bragg to be like a standard Bragg reflector with two alternating layers. We still allowed the composition and thickness of the two layer unit to change but constrained the structure

otherwise by consistently repeating this two layer unit 30 times with constant external layers. What this essentially did was allow for the center wavelength to shift as the equation n*d=lambda/4 still held and n and d were the only things allowed to vary. This reduces the number of distinct combinations (under these assumptions) to $36x10^6$. This gave an amount of information but still did not allow for a significant amount of variation from standard Bragg reflectors.

The next method tried was a 4-layer period repeated. This preserves the periodicity that allows the effect to be amplified but allows for more variance in the central wavelength and for more complex interference effects. This allowed for 10^{15} combinations.

Another system to have the same number of variables but with a different structure was two sets of Bragg reflectors, henceforth referred to as the two halves structure. In this the first 30 layers were two alternating layers, and the second 30 layers were a different set of two alternating layers. This allows for essentially two different Bragg reflectors. The idea was that this could have slight offsets that could add to a higher overall Bragg at the central wavelength with still low sidelobe reflection.

The fourth main type of Bragg reflector, the Fibonacci reflector, used was completely different and used a method developed by Ghulinyan. Ghulinyan wrote about a Bragg structure based on the Fibonacci sequence. Instead of layers A and B being repeated as AB they were AB/ABA/ABAAB/ABAABABA. The reason this works is as the structure grows you essentially have regions of AB next to each other separated by AA. Since A and B follow standard Bragg requirements, AA is a half wavelength structure and leads to destructive interference leading to what this paper terms “microcavities” between the typical Bragg reflector. This effect leads to wider Bragg reflectors with zones of high transmission which seems like it should be exactly what we want. In practicality because the high transmission zone was relatively small, the sidelobe reflection tended to still be very high compared to the peak and so this design was largely discarded. [15]

3.5 Use Of Structures and Figures of Merit In Genetic Algorithms

In order to take these structures and optimize them, the thickness and compositions of $Al_xGa_{1-x}As$ of all structures except the Fibonacci structures were varied. In the Fibonacci structure, only the compositions and the central wavelength were varied. In order to set up a genetic algorithm a few parameters are necessary. Primarily, the variables that the algorithm is varying, the equation that relates the input to the output (the figure of merit), whether the output is maximized or minimized,an initial condition and a range in which the inputs can vary. This tells the genetic algorithm how to optimize and what range it can optimize in. The different structures essentially dictate the variables, and the figures of merit describes the output. For instance for the 4 layer periodic Bragg I would allow 4 thicknesses and 4 compositions to change and then run through a function that produced the reflection, current or power which was either maximized or minimized as appropriate. The input variables of thickness and composition as well as whatever the output is are then saved and can be used to construct whatever analysis is desired.

CHAPTER 4

DATA

The following section summarizes the modeling work done to understand Bragg reflectors in solar cells. In particular, it analyzes how closely the models I worked on matched reality and the optimizations I conducted, iterating the complexity and accuracy of the figure of merit and testing the impact of EQE and Vop on the cell structures.

4.1 Validity of Models

A crucial check for any model is to ensure it is consistent with real-world results. These checks were done at varying levels of model complexity to ensure that each new set of assumptions in the model were accurate. Since it is impractical to measure every conceivable compound of AlGaAs, material models were used instead of experimental results. The index of refraction(n) and extinction coefficient(k) of the models were compared against their experimentally measured counterparts. Another test measured the reflectance of an actual Bragg reflector and compared that measurement to a model that allowed the thickness and composition to vary to fit the measured reflectance as closely as possible. Some work was done to compare the overall cell external quantum efficiency(EQE) to the measured cell EQE, but this work was not as rigorous. It is essential to compare the models at each step because as complexity increases, the models lose fidelity.

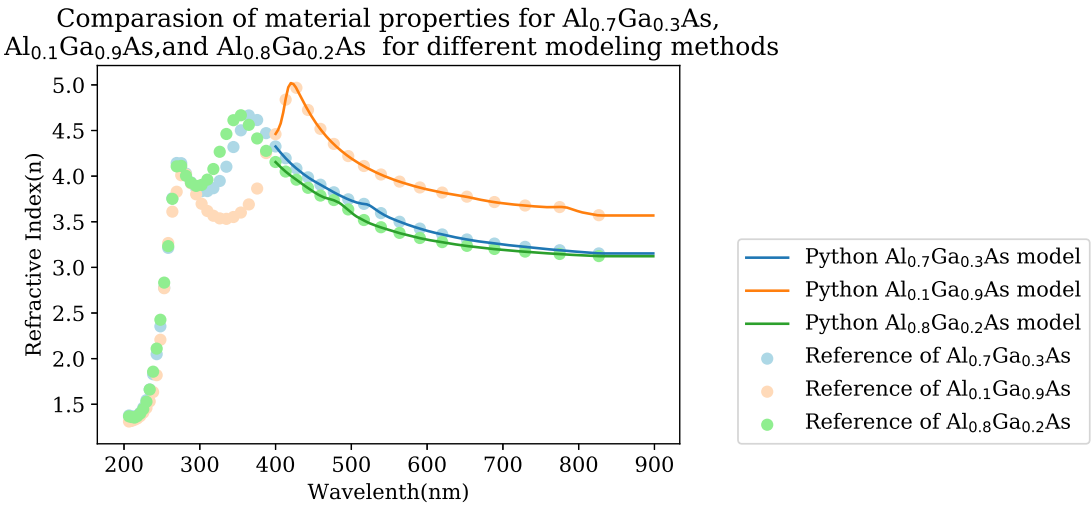

Figure 4.1 Comparison of measured and modeled $Al_xGa_{1-x}As$ materials

The most basic test done compared the index of refraction of the modeled Al_xGa_xAs with the corresponding experimental index of refraction, as shown in Figure 4.1. While other materials besides $Al_xGa_{(1-x)}As$ were used, their material properties were measured while $Al_xGa_{(1-x)}As$ was modeled so it was the only material necessary to check. The reliability of the modeled materials is remarkably consistent with the measured materials through the entire range and gives confidence to the assumption that the materials modeled are functionally identical to the materials that would be used. Figure 4.2 is a model of the reflection of a Bragg reflector grown using metalorganic vapor-phase epitaxy(MOVPE). MOVPE is a technique for growing optoelectronic structures by flowing gases of requisite materials into a reactor chamber, where they deposit onto the substrate as the final structure. Growing different materials can be grown by changing the deposition materials and conditions such as the pressure, temperature and flow rate, which will change the vapor pressure and reaction rate, which will, in turn, impact the final material.

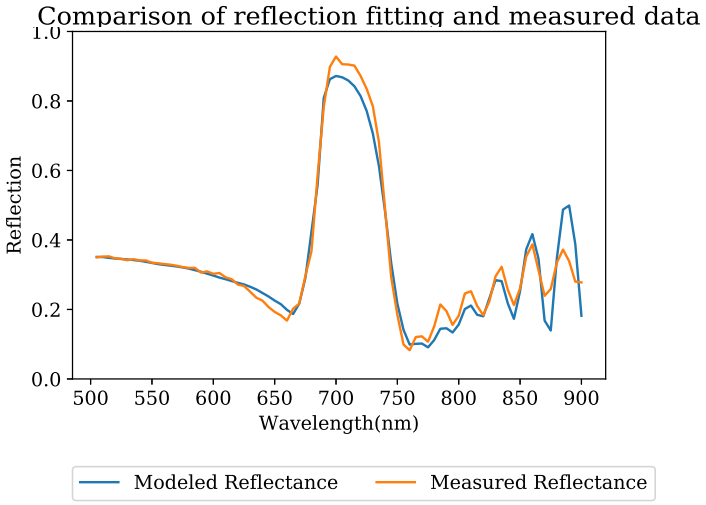

Figure 4.2 Comparasion of measured and modeled Bragg reflector

In order for the two disparate types of materials to react at the same reaction conditions, the precursors are used such that when they break down they produce free radicals that facilitate the reaction of the final substrate. [22]

The system input was a 60 layer Bragg consisting of 30 repeating units of 28.3 nm of $Al_{0.1}Ga_{0.9}As$ and 101.6 nm of AlAs with a GaInNAs back. This GaInNAs layer served as an absorbing layer, so the behavior of the reflection of the Bragg reflector could be analyzed with minimal impact from the back contact. The nominal thickness input into the reactor and the actual thickness are not likely to be identical, so a local genetic algorithm BOBYQA was used instead to change the thickness and composition to better reflect the actual growth conditions by minimizing the mean square error. The model was found to be 38.5 nm of $Al_{0.01}Ga_{0.99}As$ and 66.3 nm of $Al_{0.7}5Ga_{0.25}As$. While there is a significant difference, this reflection measurement was taken from near the edge of the sample, where the deviations in thickness and composition were greatest. This model is not perfect, both in the solutions outside of the range that we would reasonably expect and in the reflection profiles not matching correctly. There are several possible explanations for these discrepancies knowing that the bulk of the material is from our previously tested AlGaAs, including rough approximations of the compositions of the GaInNAs back contact

and an unknown and unaccounted for input light angle. However, one primary source of error is that changing the composition and changing the thickness have essentially the same effect of altering the peak location, and so one reflection profile was insufficient to produce one unique solution.

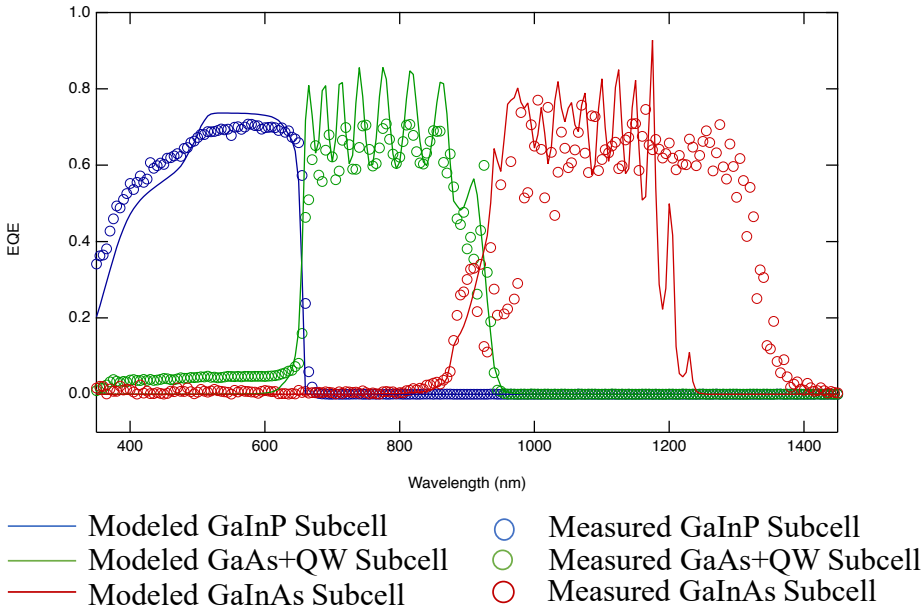

Figure 4.3 Modeled cell design compared to measured cell with InP model

Figure 4.3 is a comparison of the measured and modeled EQE of MQ689. Unsurprisingly this model is the least precise as it has the most assumptions built into it. The model I built assumed eight layers (plus the quantum wells), while the actual growth has 98 layers (plus the quantum wells). The assumption that the other 90 layers did not significantly contribute, plus the discrepancies between modeled material properties and physical material properties, are the likely causes of the modeled and measured EQE discrepancies. In particular, the cutoff wavelength of the modeled GaInAs subcell is much lower than the measured cutoff frequency (1200 nm Vs. 1400 nm), which leads me to believe the material model of GaInAs used had a different bandgap than the GaInAs that was grown. The primary region of interest is 800 nm to 1100 nm, as that is where the effects of the Bragg reflectors are generally most prominent. The reflection of the sidelobe

reflection will have mostly tapered off after 1100 nm, so it is a less significant loss than loss in the 800 to 1100 nm range.

4.2 Influence of Number of Repetitions, Thickness of Layers, and Composition of Layers on Bragg Reflection Profile

While the most fundamental check of the models is their ability to match reality under known conditions, another good reality check is to compare the trends with the equations that govern them. The impact of the number of periods, thickness, and composition on the reflectance are well defined in the math. Therefore, modeling the impact of changing any of these variables allowed us to compare the equations that govern the reflectance while also allowing us to gain a more intuitive sense of the impact of these factors. To understand these factors, a calculated 1/4 wavelength Bragg reflector composed of 65.1 nm of $Al_{0.1}Ga_{0.9}As$ and 78 nm of AlAs was modeled, and then alterations were made from that base structure. This model matched the dropoff wavelength of the Bragg reflector with the wavelength at which the GaInAs subcell increased.

4.2.1 Number of Repetitions

The peak reflection equation of a two-layer 1/4 wavelength Bragg reflector is:

$$R = [\frac{n_1^{2N} - n_2^{2N}}{n_1^{2N} + n_2^{2N}}]^2 \tag{4.1}$$

In equation 4.1 n_1 is the index of refraction of the first material, n_2 is the index of refraction of the second material, and N is the number of iterations. Plotting this equation as a function of the number of iterations reveals that as N increases, so does the reflection, but the derivative approaches 0. This derivative is because the increase in reflection due to the addition of a period is less significant as the overall thickness approaches optical thickness. Figure 4.4 takes the 1/4 wavelength Bragg calculated previously(65.1 nm $Al_{0.1}Ga_{0.9}As$ and 78 nm AlAs) and shows the expected trend as the difference between each additional layer decreases.

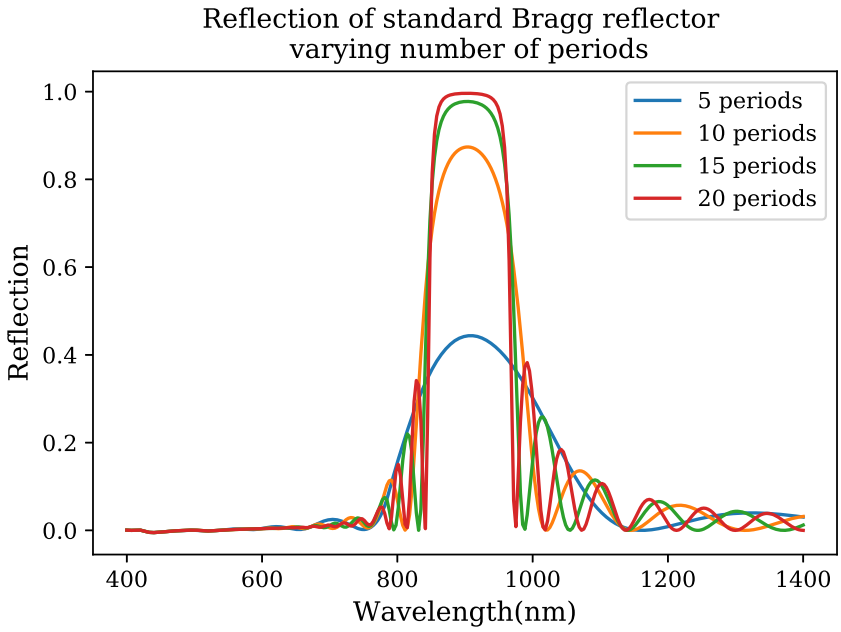

Figure 4.4 Reflection from Bragg reflector with different number of periods

4.2.2 Thickness of Layers

The thickness of each layer changes the overall composition because it essentially shifts where the central wavelength is. Since n*d=λ/4, if d changes, so will λ, the central wavelength.

Below 800 nm, $Al_{0.1}Ga_{0.9}As$ has a non-zero absorption coefficient and so photons are lost to absorption. Figure 4.5 shows what one would expect for all Bragg reflectors above 800 nm: a series of Bragg reflectors essentially identical except for an offset. This absorption does not significantly impact our results as only Bragg reflectors used for demonstrative purposes had significant reflectance below 800 nm.

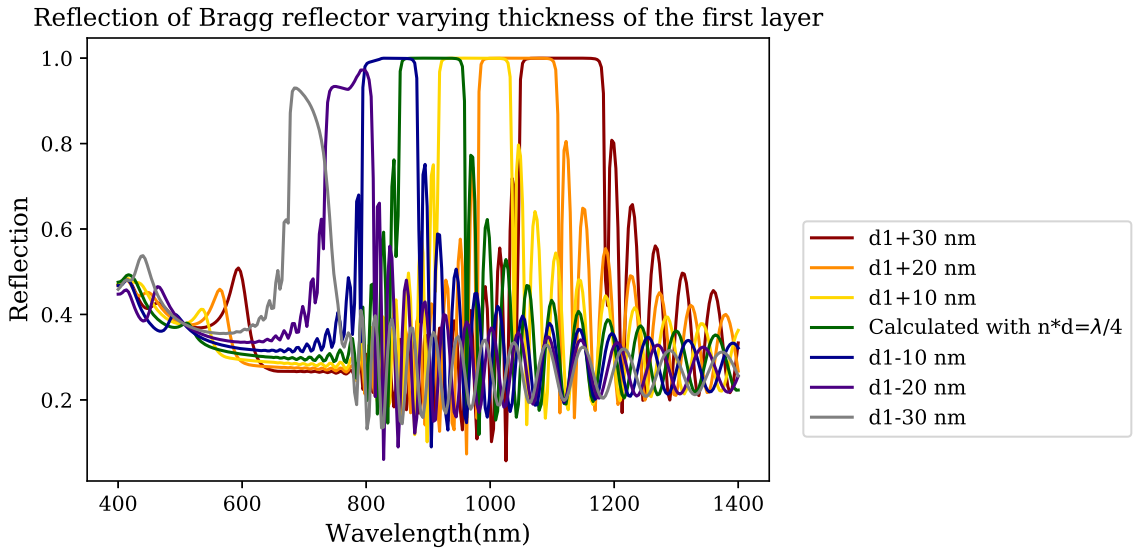

Figure 4.5 Change in reflectance of Bragg reflector from first thickness

4.2.3 Composition of Layers

The reflection profile for Bragg reflectors with a changing composition of the first layer shows a very similar trend to the reflection profiles where the thicknesses were altered. This is because n*d=λ/4 is still applicable. The change is less direct as a change in material composition leads to a change in the index of refraction that then leads to a shift in the wavelength. This multi-step process leads to a decrease in impact to the central wavelength, as shown in Figure 4.6. As the aluminum content increases, the contrast between the layers decreases, leading to less reflection per layer interface and, therefore, more layers are required for the same peak reflection.

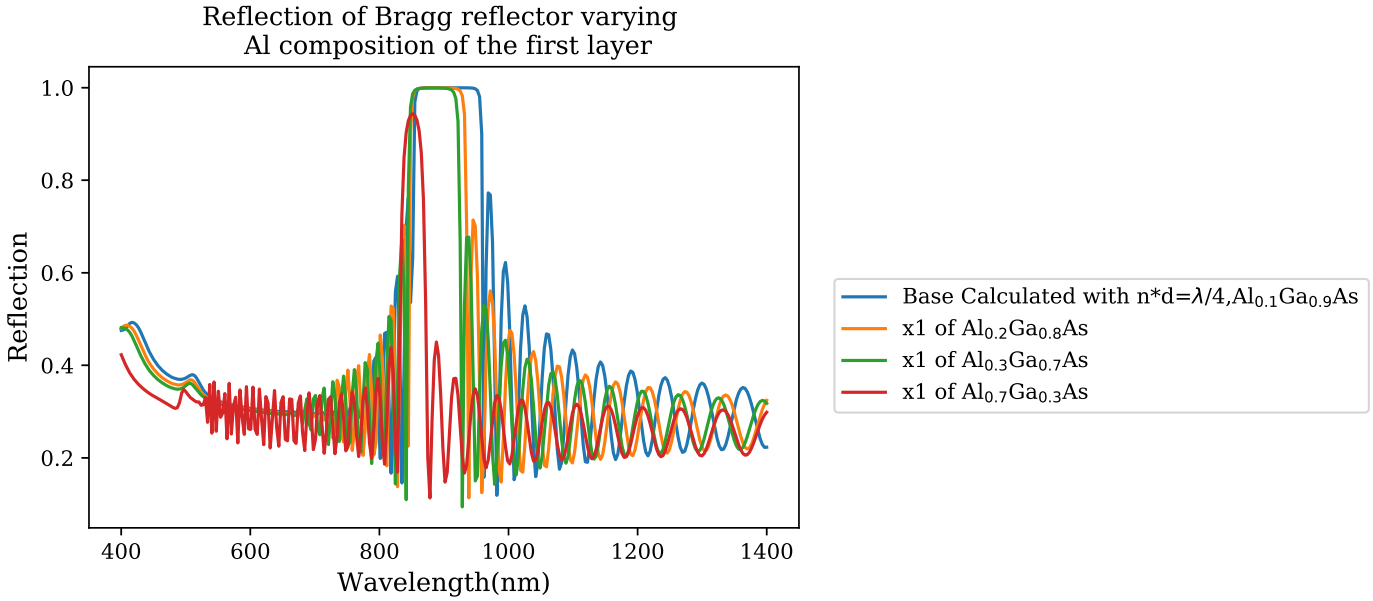

Figure 4.6 Impact of composition

4.3 Influence of Number of Quantum Wells and Vop of GaInAs Subcell on Power of GaAs+QW and GaInAs Subcells

All the Bragg reflectors here were used for understanding, so all are two layers repeating 30 times for a total of 60 layers. Table 4.1 illustrates the components of each layer. The 1/4 wavelength Bragg reflector was calculated at a 930 nm central wavelength with $Al_{0.1}Ga_{0.9}As$ and AlAs, the maximized R was an optimization done to find the highest reflection at 930 nm and the maximized T after 930 nm was an optimization done to find the highest transmission after 930 nm that still had a reflection at 925 above 0.7.

Table 4.1 Structure of Bragg reflectors compared

	1/4 λ	**Rudimentary Optimization**	**Maximized R at 930 nm**	**Maximized T after 930 nm**
Material 1	$Al_{0.1}Ga_{0.9}As$	0<x1<1	$Al_{0.1}Ga_{0.9}As$	$Al_{0.82}Ga_{0.18}As$
Material 2	AlAs	0<x2 <1	AlAs	$Al_{0.23}Ga_{0.77}As$
Thickness 1(nm)	63.0	40<d1 <100	42.06	100
Thickness 2(nm)	75.5	40 <d2 <100	100	40

4.3.1 Impact of Vop of GaInAs on Trends of Overall Power

The equation used to find the power of these subcells was

$$P = Vop_{GaAs+QW} * Jsc_{GaAs+QW} * FF + Vop_{GaInAs} * Jsc_{GaInAs} * FF \tag{4.2}$$

In a given circuit, power is traditionally found as the voltage times the current. However, in a solar cell, since the voltage and current are dependent on the state of the circuit, no one number defines the power under every condition. Since the open-circuit voltage and the short circuit current represent the maximum voltage and current respectively, and the fill factor represents the ratio of the difference between ideal maximum power and actual maximum power, those three values multiplied together represent the maximum power of the cell, which can be used as an effective metric. In series-connected multijunction cells, this is not a good metric because they are limited by the lowest current of any subcell, but this factor is irrelevant for a multi-terminal device. In order to give ourselves more freedom and hopefully a deeper understanding of the phenomenon without the lower current potentially eliminating other solutions, we calculated the sum of the power without considering current matching.

As the reflectance of the Bragg changed the absorbance of the cell, it significantly impacted the current in each sub-cell but had no substantial impact on the Vop, which is a stronger function of material quality and bandgap. Therefore, the model used in pyphotonics with the GaInAs material used was only one of many potential back subcells. To better understand the material's impact, the Vop on the overall cell design a series of models with different open circuit voltages were run and analyzed.

Figure 4.7 summarizes the findings where each power was divided by the power of the subcells with no Bragg reflector at that Vop. This was because as the Vop of the GaInAs increases so will the overall power in a linear fashion. This is not a particularly insightful result and can obscure the more subtle trends of the comparison of the types of Bragg reflectors over time. As the figure stands, it is possible to see that the optimized reflection

is always higher than no Bragg, which is a good sign, but the difference becomes less significant as the Vop increases. This makes sense in that a bigger proportion of the power comes from the GaInAs as the Vop increases so that the Bragg will be less beneficial. As the Vop increases the GaInAs subcells contribution to the power, this idea is more critical. This explains the general trend of minimized transmission consistently having the highest power, a difference that only increased as the Vop did as the loss due to reflection away from the GaInAs subcell was the least. Similarly, you can see that maximizing reflectance was more favorable than the 1/4 wavelength design that was not optimized one way or the other when the Vop of GaInAs was low and increasing the GaAs power was more important but then crosses over than 0.35 V. This trend of highest to lowest power generally also reflects a specific preference for lower transmission above improving the bragg that only increases as the Vop is increased.

Figure 4.8 is a more detailed analysis of this. The left-hand graph shows the power of the GaAs+QW subcells with the maximized reflectance and 1/4 wavelength Bragg with the highest power, then maximized transmission and then no Bragg. The optimized Bragg power decreases as the Vop increases, which makes sense as it becomes less important to increase the power of the GaAs+QW subcell and more critical to not lose power in the GaInAs subcell. The GaInAs subcell shows almost the opposite behavior. This makes sense as the optimized Bragg and 1/4 wavelength was designed to maximize the GaAs+QW regime, which it does, and the maximizing transmittance Bragg was designed to minimize the power loss in the GaInAs subcell, which it also does. The trend of the optimized of Bragg reflector slopes down in the power of the GaAs subcell and increases in the GaInAs subcell. This makes sense in that the Bragg reflector trends towards minimizing the loss to the back reflector the more impact that loss has on the overall power.

4.3.2 Impact of Changing Quantum Wells

The impact of changing the number of quantum wells is a bit more complex as it changes the structure of the actual cell. Figure 4.9 shows the overall trends.

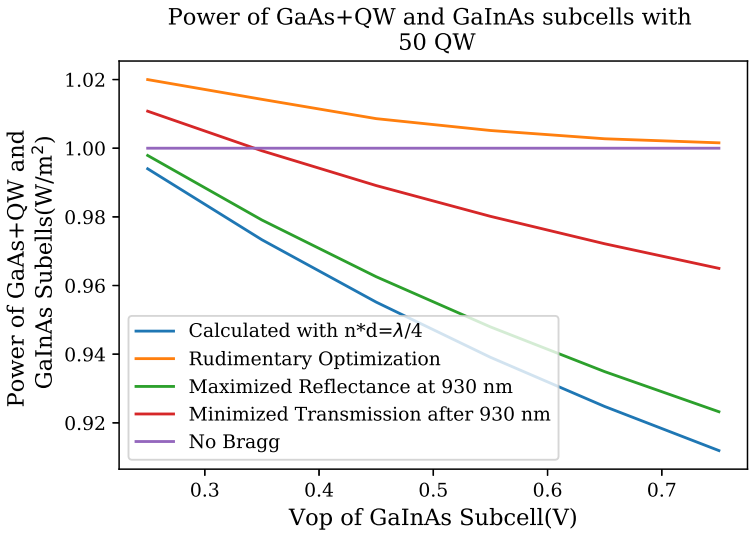

Figure 4.7 Normalized change in power as a function of the Vop of the GaInAs subcell

Figure 4.8 Impact of Vop of GaInAs on the power of GaAs+QW subcell and GaInAs subcells independently